ARTICLE NO. 79-0781R

C80-104

Crash Simulation of Composite and Aluminum Helicopter Fuselages Using a Finite Element Program

00018
80003
80006

R. Winter* and A.B. Pifko*
Grumman Aerospace Corp., Bethpage, N.Y.
and
J.D. Cronkhite†
Bell Helicopter Textron, Inc., Fort Worth, Texas

This paper describes a mathematical investigation of the crash impact responses of an all-composite helicopter cockpit section incorporating an energy absorbing concept and one of conventional aluminum construction, using the Grumman DYCAST finite element nonlinear structural dynamics computer program. The overall objective of this initial investigation was to explore the application of DYCAST to the design of future helicopter structures. The specific purposes were to assess the finite element code as a crashworthiness design analysis tool, and to compare the responses of the two fuselage sections. The results indicate that the finite element simulation is a powerful analysis tool, providing sufficient detail to evaluate individual structural components, and that the crashworthiness of an all-composite cockpit section could be enhanced with energy absorbing concepts.

Introduction

THIS work was conducted to assess the applicability of the Grumman DYCAST nonlinear finite element computer code[1,2] for crash simulation of future helicopter airframes constructed of composite materials. The effort was part of a contracted program with the Army in which Bell Helicopter Textron and Grumman Aerospace Corp. jointly surveyed and assessed available data and analytical tools to determine the crash impact characteristics of composite helicopter airframe structures. The preliminary results of the survey are discussed in Ref. 3 and the overall results appear in Ref. 4.

There are several design considerations important to the crashworthiness of the helicopter airframe structure. The two fundamental guidelines to consider are, first, that a protective shell be maintained around the occupied area during a crash and, second, that the structure be crushable and absorb energy, thus reducing decelerative forces on the occupants and hazardous large masses. Airframe structure crashworthy design considerations are summarized in Fig. 1.

In the future, innovative design configurations may be used to optimize the crash resistance of helicopter airframe structures. These configurations could provide for energy absorption and force attenuation by surrounding the protective structural shell by a crushable material such as foam, honeycomb, or a composite concept. Some typical energy absorbing concepts that might be applied to the lower fuselage structure of future helicopters are shown in Fig. 2. The crushable material in the lower fuselage should be designed to attenuate crash forces, absorb and dissipate energy, and distribute loads to the stronger primary structural shell.

A key to evaluating and optimizing the crashworthiness of helicopters is the establishment of comprehensive analysis tools to aid the aircraft designer. Designing a crash resistant structure requires an understanding of the behavior of a complex structure deforming under crash impact loads. Computer techniques are needed that will complement the linear elastic (small deflection) finite element design analysis methods presently being used, such as NASTRAN.[5] It is anticipated that in the future a structural crash simulation, such as the Grumman DYCAST computer program, can be used along with NASTRAN for airframe design analysis.

In this investigation, a typical section of fuselage structure (Fig. 3) of a troop transport helicopter was selected for analysis with DYCAST. Cockpit sections of both metal and composite construction were analyzed for comparison (Figs. 4 and 5). The section of composite construction incorporated an energy absorbing concept. Identical vertical impact conditions of 30 ft/s into a rigid horizontal surface were simulated for each section so that analytical results would be comparable. This should provide, first, an evaluation of DYCAST for crash simulation of composite as well as metallic helicopter fuselage structures and, second, an evaluation of the energy absorbing concept for enhancing the crash impact response of a composite structure.

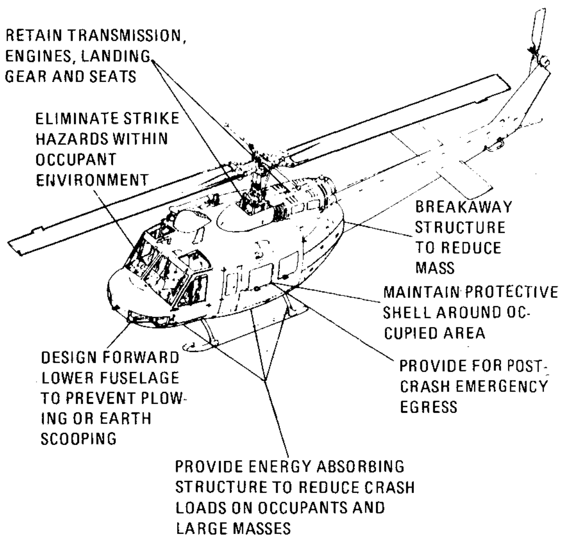

Fig. 1 Airframe structure crashworthy design considerations.

Presented as Paper 79-0781 at the AIAA/ASME/ASCE/AHS 20th Structures, Structural Dynamics & Materials Conference, St. Louis, Mo., April 4-6, 1979; submitted May 7, 1979; revision received Dec. 4, 1979.

Index categories: Helicopters; Structural Dynamics; Structural Composite Materials.

*Staff Scientist, Research Department. Member AIAA.

†Senior Structural Dynamics Engineer, Flight Technology Department.

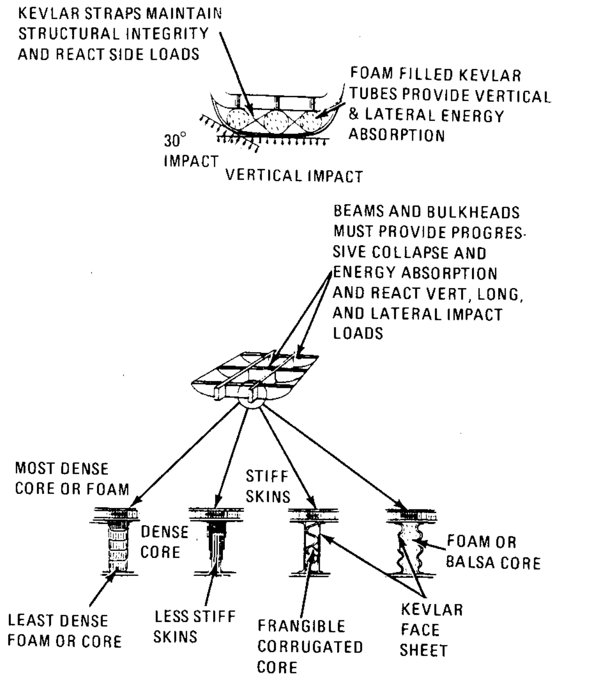

Fig. 2 Energy absorption concepts, beams and bulkheads, vertical impact.

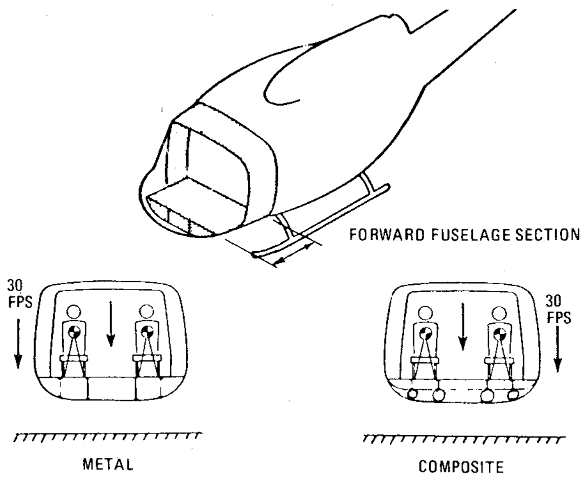

Fig. 3 Section of helicopter used for DYCAST analysis.

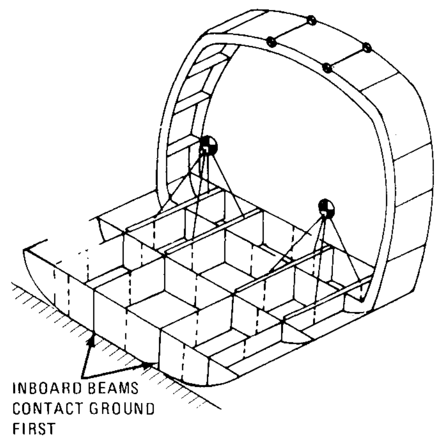

Fig. 4 Original metal section, floor panels removed.

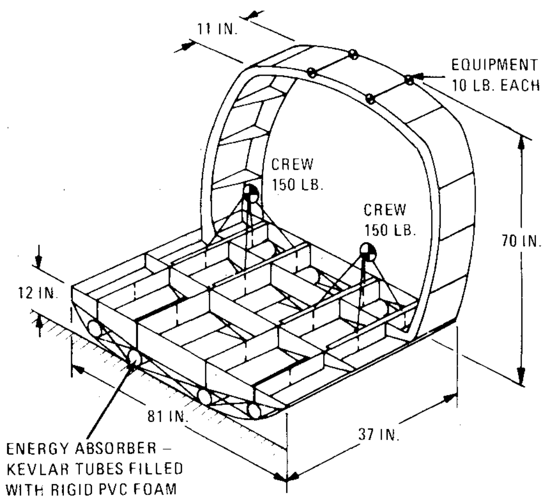

Fig. 5 Original composite section, floor panels removed.

A general description of the analysis is given here. Details of the idealized structures are presented in Ref. 4. Since nonlinear finite element crash simulations in general—and DYCAST in particular—are still in the development stage, it was decided to limit the study to a detailed model of the crew compartment fuselage structure only. No attempt was made to perform a full crashworthiness evaluation of the aircraft. A full evaluation would involve analysis of the entire energy management system of the helicopter, including the complete airframe, landing gear, and seats.

DYCAST Features

The major DYCAST features of importance to the engineer are:

1) Nonlinear spring, stringer, beam, and orthotropic thin sheet elements.
2) Plasticity.
3) Very large deformations.
4) Variable problem size.
5) Restart (stop, review, and continue).
6) Deletion of failed members.
7) Four different numerical solution methods, three with internally varied time steps.
8) Modular formulation.

The basic element library of stringers (axial stiffness only), beams (axial, two shears, torsion, and two bending stiffnesses), and isotropic or orthotropic membrane skin triangles (in-plane normal and shear stiffnesses) allows the convenient modeling of aircraft-type structure built up from such components. The nonlinear spring element is a general purpose axial stiffness unit with a user specified force-displacement curve.

The changing stiffnesses in the structure are accounted for by plasticity (material nonlinearity) and very large deflections (geometric nonlinearities). The plasticity enters the model through the nonlinear stress-strain curve for each element. The geometric nonlinearities are modeled by reforming the structure into its new shape after small time increments, while accumulating deformations, strains, stresses, and forces. In this way, the progressive crushing and folding of structural elements can be followed. The nonlinearities due to combined loadings (such as beam-column effects) are maintained, and the stiffness of the elements will vary with time, depending upon the combination of loads imposed on them.

The restart feature allows for a large problem, or one of long event duration, to be run in small time sequences. This minimizes the tieup of computer facilities, allows the user to examine the response as it progresses, and permits the ending of a simulation if a critical damage occurs.

The numerical time integrators available are fixed-step central difference, modified Adams, Newmark Beta, and

Wilson theta. The last three have variable time steps, controlled internally by a solution convergence error measurement. Thus, the time steps increase and decrease as required during the simulation.

The overall accuracy and computational cost of the simulation will depend upon the quantity of elements used (fineness of the geometric model). The finer the model, the greater the accuracy and cost.

A user oriented input/output format is utilized. The primary input data groups are: numerical controls and options; geometry (nodes and elements); motion constraints; initial conditions; rigid masses; material properties (stress-strain curves); element cross-section geometries; and applied dynamic loads (if any).

The output data are in the form of: printed displacement, velocities, accelerations, strains, stresses, and forces; plotted histories of displacement, velocity, and acceleration at chosen nodes; and time-sequenced drawings of deforming structure or portions from any viewing angle.

Actual Fuselage Sections

The fuselage sections to be modeled were defined at Bell and idealized and analyzed at Grumman. Both the conventional metal section and the all-composite section with energy absorbers were impacted vertically into a rigid horizontal surface at 30 ft/s. Note that only the central floor section between the two inboard main beams is in contact with the ground surface. The outboard fuselage is above the ground at impact.

The baseline metal section of Fig. 4 was taken from a representative troop carrying helicopter, as shown in Fig. 3, and the composite section of Fig. 5 was designed by Bell to replace it. The two cockpit sections therefore had the same overall dimensions indicated in Fig. 5 and were designed for the same flight loads. Their floor structures were composed mainly of four longitudinal beams, four transverse bulkheads, an outer belly skin, and a floor panel covering. The roof and door posts were deep channel beams built up from the thin webs and flanges with angle stiffeners at the corners and edges.

Both sections carried two 150 lb point-masses representing crew members on four rigid weightless seat legs attached to seat rails that were fastened to the top caps of the main longitudinal beams. The seat legs were positioned midway between bulkheads, just above the vertical stiffeners on the beam webs. Vertical web stiffeners are shown as dashed lines in Figs. 4 and 5.

The conventional metal section had full depth webs on the beams and bulkheads. For the composite section, the lower portion of the longitudinal beams were replaced by energy absorbing crushable tubes, and the lower parts of the bulkheads were replaced by diagonal tension straps and transverse formers attached to the skin.

The metal baseline section had titanium seat rails, 7075-T6 aluminum longitudinal beam caps, and all remaining structure 2024-T3 aluminum. The composite section had the same seat rails; ± 45 deg Kevlar/epoxy laminate for the beam webs, bulkhead webs, energy absorbing tube walls, and doorpost webs; and 0/90 deg Kevlar/epoxy laminate for the belly skin and floor cover panels. A multidirectional graphite/epoxy laminate was used for the longitudinal beam caps and transverse skin formers, while unidirectional graphite/epoxy reinforced the bulkhead caps and formed the corner angles for the door posts and roof frame. The energy absorbing tubes were filled with PVC foam and braced by the transverse diagonal tension straps of unidirectional Kevlar/epoxy.

Idealized Fuselage Sections

The idealized fuselage sections are shown in Figs. 6 and 7. For this analysis, only the left half of each section was modeled because of symmetry. Each fuselage section was broken down into its natural structural components: beam webs and caps, bulkhead webs and caps, skin panels, and energy absorbing tubes. Each of these was further divided into elements using stringers, beams, membrane triangles, and nonlinear springs.

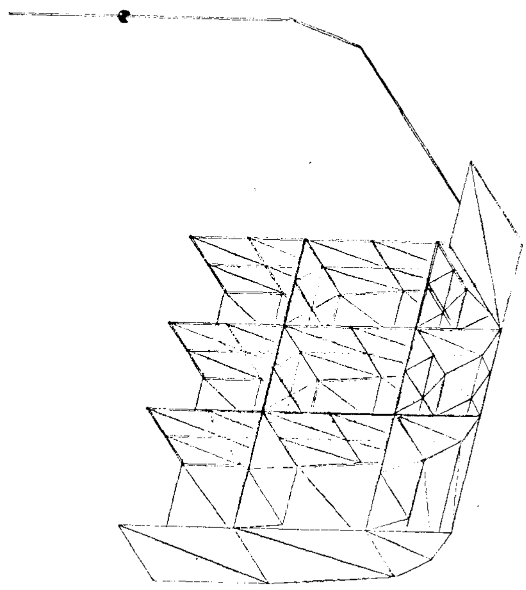

Fig. 6 Idealized baseline metal half-section, floor panels and seat deleted.

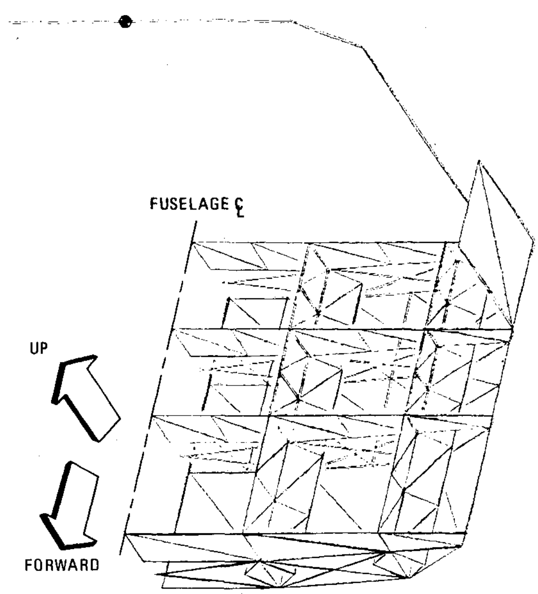

Fig. 7 Idealized composite half-section with energy absorbers; floor panels and seat deleted.

A general description of each idealized section follows. Complete details are given in Ref. 4.

Metal Baseline Section Model

In the metal baseline model, the bulkheads and longitudinal beams were generally idealized using isotropic membrane triangles for webs, and beam elements for the seat rails, web caps, and vertical stiffeners. The exception was forward of the second bulkhead, where the beam elements were replaced by stringers. This was done because local bending of caps and stiffeners was assumed to be important only near the seat and door post attachments. Generally, less modeling detail was used forward of the second bulkhead (as apparent in Fig. 6), since less load and deformation were expected there.

The roof frame and upper door post were modeled with a single arch of beam elements. The lower part of the door post was modeled in more detail, using triangles for the outer skin panel and beam elements for the frames to distribute the roof loads more evenly into the floor edge. The two 10 lb equipment masses on the roof were replaced by a single 20 lb mass with the proper value of rotary inertia.

The belly skin panels and floor cover panels were represented by membrane triangles. The floor cover is deleted from Fig. 6 to show the subfloor structure more clearly. Since the outer part of the floor structure was cantilevered above the ground, a downward bending motion was expected, imposing a compressive load on the belly skin panels which would then tend to buckle. Therefore, an equivalent beam grid was added to the belly skin panels to account for their transverse bending stiffness.

The material behavior of the aluminum and titanium used in the metal baseline section was represented by elastic-perfect plastic stress-strain curves.

The metal section model had 111 nodes, 348 elements, and 419 degrees of freedom (unknown displacements).

Composite Section Model

The composite section was idealized in the same way as the metal section, except that orthotropic membrane triangles represented all the webs, skins, and tube walls. The longitudinal bending, shear, and axial stiffnesses of the tubes were modeled by using orthotropic membrane triangles to form hollow, square-diamond tube walls that could flatten as the tubes crushed. The vertical crushing behavior of each energy absorbing tube was represented by seven vertical nonlinear springs inside each tube, whose force-displacement curves were derived from the tube crush data shown in Fig. 8. During rebound, the unloading from any peak load proceeded along the initial slope, as shown by the dashed line. The diagonal tension straps below each bulkhead were modeled by nonlinear springs having no compression load capacity; that is, they were treated as cables that would go slack when compressed.

The material behavior of the composite laminates was represented by a linear elastic stress-strain curve up to the failure stress, with no plastic deformation. The failure criterion assumed that failure would occur in an element whenever a calculated strain component exceeded a specified failure level.

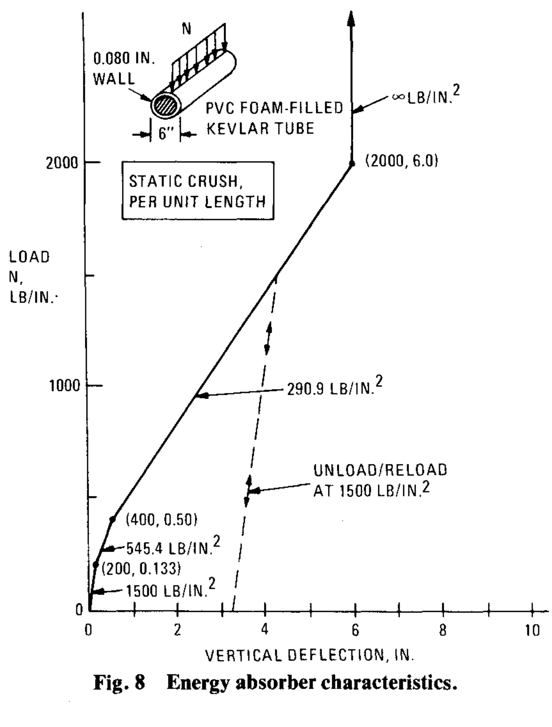

Fig. 8 Energy absorber characteristics.

The composite model contained 144 nodes, 422 elements, and 471 degrees of freedom.

Simulation Results

The primary output data for each simulation consisted of printed data at time intervals varying from 20 to 230 μs, and a digital magnetic tape of the complete motions at all the nodes at every time increment. From each tape, approximately 30 traces of displacement, velocity, and acceleration histories were automatically machine-plotted for certain selected nodes, including the crew and equipment masses.

From the same tapes, approximately 100 machine drawings were generated showing the deformed state of each structure at many time intervals for different views. These views included several of the entire structure, plus one each of the major subsections (bulkheads, main beams, skin panels, etc.). In this way, a comprehensive qualitative and quantitative display of the structural response was available for both simulations. The data reported here are necessarily restricted to a small part of the total.

The metal baseline simulation covered 10 ms of event time, with 71 time steps, using 19 min of computer time (CPU) on an IBM 370/168. The composite model simulation covered 30 ms, with 197 time steps, using 56 min of CPU time. The Newmark-Beta numerical time integrator option with the capability of variable time steps was used in both cases.

Metal Baseline Section Results

The most significant events during the impact simulation for the metal baseline section are listed in Table 1.

Very little deformation of the subfloor structure was noticeable, but the roof beam deformed downward while the vertical door post buckled outward. There was also a slight forward buckle of the middle web on the aft bulkhead.

The vertical motion histories of the rigid crew/seat mass are presented in Fig. 9. It developed a large short-duration upward acceleration pulse, and a small peak downward displacement of only 0.23 in. out of a total floor structure depth of 12 in. It is apparent that the floor structure is very stiff for this rigid crew mass in this impact condition. The large accelerations cannot be used directly to evaluate crew response because of the rigid seat. However, it could have been possible to use the histories of displacement (or ac-

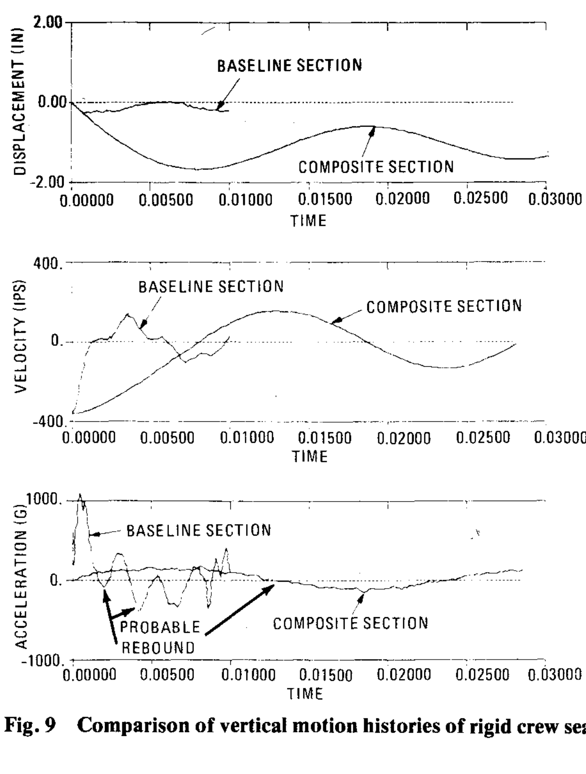

Fig. 9 Comparison of vertical motion histories of rigid crew seat.

Table 1 Events during impact simulation for metal baseline section

Time, ms	Event
0.1	Plastic compression in main beam under inboard seat legs
0.5	Crew/seat mass peak acceleration, plastic bending in seat rail under inboard legs
1.3	Crew mass maximum downward displacement 0.23 in., plastic bending in upper door post
2.0	Slight plastic buckle of belly skin panels, plastic tension of floor cover panels, vertical oscillations of equipment mass begin
2.4	Plastic bending in roof frame at equipment mass
7.4	Door post buckle begins
7.9	Upper door post local bending failure
10.0	End simulation

Table 2 Events during impact simulation for composite section

Time, ms	Event
4.9	Local bending overstress in top cap of inboard main beam under seat legs
5.0	Slight buckle of belly skin panels
8.0	Crew mass peak acceleration
8.4	Maximum 1.67 in. downward displacement of crew mass and floor structure, maximum crush of inboard tube, outer tube barely contacts ground, slight forward buckle of bulkheads under seat
10.2	Bending failure in roof frame
15.4	Maximum 4.1 in. downward displacement of overhead equipment mass
30.0	End simulation

celeration) at the four seat leg attachments as input data to a separate, uncoupled, seat/occupant model, but that was beyond the scope of this project.

The vertical oscillations of the crew mass were in phase with those of the outboard portion of the floor that was initially above the ground plane. The entire section was vibrating in bending at approximately 125 Hz, in a mode by which the outboard edge oscillated vertically while the inboard structure near the centerline remained nearly stationary. The outboard floor structure did not contact the ground.

There was some plastic deformation under the inboard seat legs in the webs, caps, and vertical stiffeners of the inboard main beams, but not enough plastic collapse to use the energy absorbing potential of the aluminum.

At 7.9 ms the vertical door post beam exhibited an excessive plastic tensile strain in the outer rear corner of its cross-section that was greater than the elongation-to-failure of 18% for the 2074-T3 aluminum. Although this local bending failure of the vertical post was indicated at its point of maximum outward deformation, the affected door post beam elements were not deleted since that action would have entirely disconnected the roof mass from the structural model. In reality, the roof structure extends rearward from the single beam arch used here, and therefore the prediction of roof collapse with this simplified demonstration cannot be considered definite for the complete fuselage. However, the restricted model used here does demonstrate the level of detail available in DYCAST and how it can be used to predict failures of individual components. The roof mass bulged downward 2.5 in. and had not yet reached its maximum deflection when the simulation was ended because of the earlier collapse of the door post.

Composite Section with Energy Absorbers

The significant events for the composite section are listed in Table 2.

A view of the deformed lower floor substructure is shown in Fig. 10, near the moment of maximum downward displacement of the crew and maximum crush of the inboard tube. Only the deformed belly skin, energy absorbing tubes, and main beams are shown. The inboard tube can be seen to be slightly flattened, while the outboard tube remains undeformed. Most of the diagonal tension straps were slack all

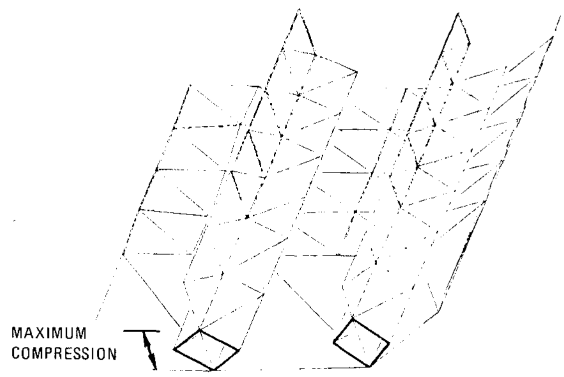

Fig. 10 Composite section skin, beam, and tube deformations at 8.2 ms (near peak crew displacement).

of the time except for those extending from the top of the inboard tube downward to the bottom of the outboard tube. Note the vertical buckling of the belly skin panels.

The horizontal roof frame was subjected to bending overstresses along its entire length, and its collapse was therefore indicated. However, it must be noted, as in the case of the metal section, that the unmodeled fuselage structure aft of the front door post would have strengthened the door post and roof frame.

Figures 11 and 12 show a set of left-side views of the inboard main beam and tube assembly, with attached inboard seat legs and crew mass. The peak vertical crush of the tube increased linearly from 0.9 in. at the front to 1.8 in. at the rear, out of an initial undeformed depth of 6.0 in. This deformation can be clearly seen in Fig. 11, in which the deformed and undeformed views are superimposed relative to the common ground surface. In Fig. 12, the same two views are superimposed so that the main beam webs coincide. This shows that very little deformation took place in the main longitudinal beam, and that the downward motions were almost entirely accounted for by the crushing of the energy absorbing tube.

The floor structure above the crush tubes remained intact except for local bending failures of the graphite/epoxy inboard main beam top caps directly under both inboard seat

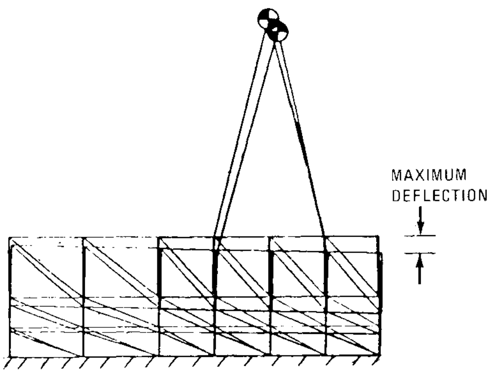

Fig. 11 Composite inboard beam and tube at 0 and 8.2 ms superimposed at ground.

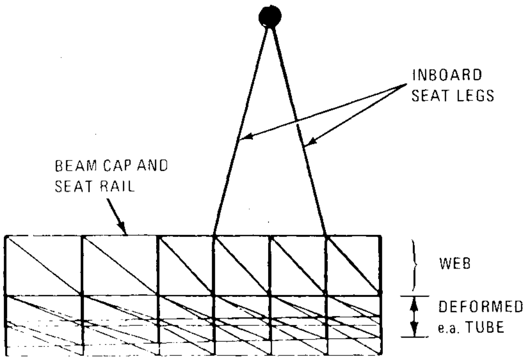

Fig. 12 Composite inboard beam and tube at 0 and 8.2 ms superimposed at crew seat.

legs. However, the beams were held together by the inboard titanium seat rail that deformed plastically at those points. Evidently, the vertical web stiffeners under the seat legs, formed by offsets of the web laminates, were insufficiently stiff and transmitted only a small share of the vertical load from the seat legs. This caused too much vertical load to be carried by bending of the longitudinal beam cap and seat rail. The addition of separate vertical web stiffeners at these positions should eliminate the beam cap failures.

The vertical motions of the 150 lb crew masses in the composite section are given in Fig. 9. The response was generally slower, with more deflection and less acceleration than for the metal section. After the initial peak vertical displacement, an oscillation cycle of 49 Hz appeared, centered on a mean displacement of 1.02 in. This compares closely to the calculated natural frequency of 51 Hz for a simple mass-spring model, using the 208.5 lb total model weight and the 55,500 lb/in. average elastic spring constant of the energy absorbing tube in its unloading-reloading mode.

Thus, it seems that the upper floor structure moved in a nearly rigid manner. The inboard energy absorbing tube initially crushed less than 23% (averaged over its length) of its total available stroke, then behaved as an elastic spring causing vertical oscillations of the floor structure and seat mass. This was not surprising, since the unloading-reloading behavior of the crushable tubes was specified as linear. If the higher frequency accelerations over 500 Hz could be neglected, then the peak value would have been 150 *g* at 6 ms.

The motion of the 20 lb overhead equipment was also slower with more deflection and less acceleration, than in the metal section, because of the crush tube behavior.

Evaluation of Responses

Comparison of the dynamic responses of the composite section with the baseline metal section indicated that, for the 30 ft/s vertical impact condition:

1) The floor structure of the metal baseline section was very stiff for this condition and did not significantly utilize the plastic deformation energy absorbing potential of the aluminum. However, the addition of engine and transmission weight would have affected this behavior.

2) The composite section transmitted smaller accelerations to the crew and equipment masses by a factor of 6 because of the crushing action of its energy absorbing tubes.

3) Less than 13% of the energy absorbing capacity of the crushable tubes was used. However, in a more complete model of the entire fuselage, including the heavy engine and transmission masses, more crushing of these tubes would occur.

4) Both sections experienced collapse or failure of the door post/roof frame arch supporting the overhead equipment mass, but this might not occur in a more complete model of the fuselage.

5) A partial local failure occurred under the inboard seat legs in the composite section, which could probably be prevented by the addition of vertical stiffeners to the beam web under the legs.

It appears that both fuselage sections contained very stiff floor structures. The composite section, however, benefited greatly from the greater compliance and the energy dissipation of the crush tubes. It seems logical, then, that the baseline metal section could also benefit greatly from the addition of such energy absorbing devices. It would have been useful to have compared the behavior of both fuselage sections with and without the energy absorbers, but that was beyond the scope of this demonstration study.

It should be pointed out that this simulation did not permit for a free rebound from the impacted surface. Rather, the structure was held to the impact surface throughout the analysis. It is likely that a free rebound would have occurred in these cases after the accelerations (Fig. 9) on the rigid crew/seat mass became negative (downward), indicating that the ground was pulling down on the structure. Thus, the structural motions after 1.6 ms for the metal and 13.0 ms for the composite sections were not realistically predicted.

The conclusions made here regarding the initial peak accelerations and displacements would probably have not been changed with rebound, because those occurred before any possible rebound. However, the peak relative displacement between a nonrigid crew/seat and the floor structure would be increased by rebound. This would increase the stroking requirements for an energy absorbing seat. The metal floors would have had more rebound velocity than the composite floor, because of the absence of any special energy dissipating design.

Conclusions

The results of this analytical demonstration indicate that the DYCAST nonlinear finite element computer program has the potential for analyzing the crash impact behavior of composite as well as metal helicopter airframe structures. The main conclusions in the assessment of DYCAST as a design analysis tool are:

1) Detailed dynamic responses were predicted, including behavior of individual components, indicating local failures and overloaded attachment points.

2) Computer effort (CPU) was acceptable for this problem. Larger, more complete structures would be more difficult to analyze, but the use of modeling detail only in limited regions of expected damage should keep computational effort at a moderate level.

3) Immediate improvements needed are rebound from the barrier surface and automatic material failure (both have now been incorporated). Future developments should include the addition of a core-sandwich plate element and a simple flexible occupant model (both are in progress).

4) Correlation and verification testing of actual helicopter-type structures needs to be conducted to validate the computer program.

The analysis indicated the potential for composite structures to be made crashworthy when configured with innovative design concepts to control dynamic loads imposed on the primary fuselage. Thus, the use of advanced composite materials in helicopter fuselages need not prevent improvements in the crashworthiness of the structure.

The element sizes of the fuselage sections analyzed in this study are probably as coarse as should be used in order to preserve an adequate representation of the structural response and failure modes.

Other important aspects such as relative cost, flammability, and toxicity of composite structures compared to metallics were not considered here, but might be important factors in the crashworthy design of future helicopters.

Acknowledgments

Work described in this paper was performed under Contract DAAJ02-77-C-0062 with the U.S. Army Research and Technology Laboratories (USAAVRADCOM), Applied Technology Laboratory, Ft. Eustis, Va. The development of DYCAST is partially supported by the NASA Langley Research Center under a joint NASA/FAA program in aircraft crashworthiness (Contract NAS1-13148).

References

[1] Armen, H., Pifko, A., and Levine, H., "Nonlinear Finite Element Techniques for Aircraft Crash Analysis," *Aircraft Crashworthiness,* University Press of Virginia, Charlottesville, Va., 1975, pp. 517-548.

[2] Winter, R., Pifko, A.B., and Armen, H., "Crash Simulation of Skin-Frame Structure Using a Finite Element Code," SAE Paper 770484, SAE Business Aircraft Meeting, Wichita, Kan. April 1977.

[3] Conkhite, J.D., Haas, T.J., Winter, R., Cairo, R.R., and Singley III, G.T., "Investigation of the Crash Impact Characteristics of Composite Airframe Structures," paper presented at 34th Annual National Forum of American Helicopter Society, Washington, D.C., May 1978.

[4] Cronkhite, J.D., Haas, T.J., Berry, V.L., and Winter, R., "Investigation of the Crash-Impact Characteristics of Advanced Airframe Structures," Report USARTL-TR-79-11, U.S. Army Research Technology Laboratories, Ft. Eustis, Va., Sept. 1979.

[5] McCormick, C.W., *The Nastran User's Manual,* NASA SP-222(03), Computer Software Management and Information Center (COSMIC), Barrows Hall, University of Georgia, Athens, Ga., March 1976.